Experimental Study on the Grinding Anisotropy of Nickel-based Single Crystal Superalloy

Ming Cai [a*], Yadong Gong [b], Yao Sun [c], Shuoshuo Qu [d], Yuying Yang [e]

School of Mechanical Engineering and Automation, Northeastern University, Shenyang, China

[a] caiming199004@126.com, [b] gongyd@mail.neu.edu.cn, [c] sy547515291@163.com, [d] qushuoshuo@163.com, [e] yyyingneu@163.com

Keywords: nickel-based single crystal superalloy DD5; grinding; anisotropy; grinding force; subsurface; grinding debris

Abstract. In order to investigate the influence of nickel-based single crystal superalloy DD5 anisotropy on grinding force, the single factor experiment was carried out. First of all, the shear modulus $G_{(001)}$ and elastic modulus $E_{(001)}$ calculation formulas of nickel-based single crystal superalloy (001) crystal plane under different crystal orientations were deduced. Then, the experimental study on the influence of nickel-based single crystal superalloy DD5 anisotropy on grinding force was conducted. Finally, the subsurface morphology after grinding and grinding debris morphology were observed. The results show that: the shear modulus $G_{(001)}$ and elastic modulus $E_{(001)}$ change periodically with the cycle of $\pi/2$. The tangential grinding force Ft is minimum when θ is 45° and the normal grinding force Fn is minimum when θ is 0°. The plastic deformation layer of about 3μm and the machined hardening layer of about 1μm appear on the grinding subsurface. The grinding debris mainly shows discontinuous and presents the serrated features.

Introduction

Grinding is one of the main machining methods in the mechanical processing field that can produce the best surface quality and the smallest dimensional error. It is generally used as the final process of the machining process to generate the final working surface of the part. The research object of this paper is nickel-based single crystal superalloy DD5 material, which is an important material for blades of aero-engine and gas turbine. It is a typical difficult-to-machine material. The whole material has only one grain, eliminating the grain boundary which generates crack sources easily. Therefore, its high temperature mechanical properties have been significantly improved. The biggest characteristic of single crystal material from polycrystalline material is that the single crystal material shows significant anisotropy within the material. The anisotropy characteristic of single crystal material has a certain influence on the grinding process, which is manifested in the grinding surface quality and grinding force, etc.

Scholars have conducted some researches on the grinding [1-3] and machining [4-6] process of nickel-based superalloy, and the anisotropic characteristics of single crystal materials [7-8]. However, there are few reports focusing on the grinding anisotropic characteristics of nickel-based single crystal superalloy. In view of the increasing application prospect of nickel-based single crystal superalloy in aerospace and national defense field, the grinding force experimental study of nickel-based single crystal superalloy DD5 was conducted in this paper. It may provide a theoretical basis for studying the grinding mechanism of nickel-based single crystal superalloy.

Grinding anisotropy experiment

Shear modulus and elastic modulus of nickel-based single crystal superalloy. Nickel-based single crystal superalloy has a typical face-centered cubic structure (FCC). According to the symmetry of the crystal structure, the shear modulus calculation formula of nickel-based single crystal superalloy in either direction is shown in Eq. 1.

$$G^{-1}=S_{44}+4\left[(S_{11}-S_{12})-\frac{1}{2}S_{44}\right]\left(\alpha^2\beta^2+\beta^2\gamma^2+\gamma^2\alpha^2\right) \tag{1}$$

In the equation: G is the shear modulus of nickel-based single crystal superalloy. α is the direction cosine of a certain crystal orientation that is relative to the x-axis of nickel-based single crystal superalloy. β is the direction cosine of the crystal orientation that is relative to the y-axis. γ is the direction cosine of the crystal orientation that is relative to the z-axis. S_{11}, S_{12} and S_{44} are the flexibility coefficients of nickel-based single crystal superalloy.

The direction cosine expressed by the crystal plane indices of nickel-based single crystal superalloy (FCC crystal) is shown in Eq. 2.

$$\begin{aligned}\alpha&=H\Big/\sqrt{H^2+K^2+L^2}\\ \beta&=K\Big/\sqrt{H^2+K^2+L^2}\\ \gamma&=L\Big/\sqrt{H^2+K^2+L^2}\end{aligned} \tag{2}$$

In the equation: [*hkl*] is a certain crystal orientation in the coordinate system. H, K, L are its specific parameters.

According to the nickel-based single crystal superalloy crystal structure characteristics of the (001) crystal plane, it is assumed that γ= 0. [*hkl*] is [*hk0*]. The shear modulus of any crystal orientation in the (001) crystal plane can be changed from Eq. 1 to Eq. 3.

$$\begin{aligned}G_{(001)}^{-1}&=S_{44}+4\left[(S_{11}-S_{12})-\frac{1}{2}S_{44}\right]\alpha^2\beta^2=S_{44}+\left[(S_{11}-S_{12})-\frac{1}{2}S_{44}\right]\sin^2 2\theta\\ &=S_{44}+\frac{1}{2}\left[(S_{11}-S_{12})-\frac{1}{2}S_{44}\right]-\left[(S_{11}-S_{12})-\frac{1}{2}S_{44}\right]\frac{\cos 4\theta}{2}\end{aligned} \tag{3}$$

In the equation: θ is the angle between the different crystal orientations and the [100] crystal orientation in the (001) crystal plane of nickel-based single crystal superalloy.

After the derivation, the formula for calculating the shear modulus $G_{(001)}$ of different crystal orientations in the (001) crystal plane of nickel-based single crystal superalloy is shown in Eq. 4.

$$G_{(001)}=\frac{1}{\frac{1}{2}S_{11}-\frac{1}{2}S_{12}+\frac{3}{4}S_{44}-\left[(S_{11}-S_{12})-\frac{1}{2}S_{44}\right]\frac{\cos 4\theta}{2}} \tag{4}$$

It can be known from Eq. 4 that the shear modulus $G_{(001)}$ along different crystal orientations in the (001) crystal plane of nickel-based single crystal superalloy changes periodically with the cycle of $\pi/2$.

According to the symmetry of the crystal structure, the elastic modulus calculation formula of nickel-based single crystal superalloy in either direction is shown in Eq. 5.

$$E^{-1}=S_{11}-2\left[(S_{11}-S_{12})-\frac{1}{2}S_{44}\right]\left(\alpha^2\beta^2+\beta^2\gamma^2+\gamma^2\alpha^2\right) \tag{5}$$

According to the above derivation method of $G_{(001)}$, the (001) crystal plane elastic modulus $E_{(001)}$ of nickel-based single crystal superalloy was deduced, as shown in Eq. 6.

$$E_{(001)}=\frac{1}{\frac{3}{4}S_{11}+\frac{1}{4}S_{12}+\frac{1}{8}S_{44}+\left[(S_{11}-S_{12})-\frac{1}{2}S_{44}\right]\frac{\cos 4\theta}{4}} \tag{6}$$

It can be known from Eq. 6 that the elastic modulus $E_{(001)}$ along different crystal orientations in the (001) crystal plane of nickel-based single crystal superalloy also changes periodically with the cycle of $\pi/2$.

Experimental conditions and scheme. The machining and testing equipment used in the experiment are the 2M9120 multi-used grinding machine, CA20 low speed wire electric discharge machine, KISLER 9257B dynamometer, VHX-1000E super-depth microscope and Ultra Plus field emission scanning electron microscope. The grinding wheel used in the experiment is made of CBN with a diameter of 180mm, whose particle size is 180#, the width is 5mm, the thickness is 5mm, and the binder is resin with a concentration of 100%. The material used in the experiment is nickel-based single crystal superalloy DD5, which is widely used in aerospace and national defense field.

The CA20 low speed wire electric discharge machine was used to cut the nickel-based single crystal superalloy DD5 (001) crystal plane specimen into a circular piece with a diameter of 55mm and a thickness of 2mm. Then crystalline division was conducted after the [100] crystal orientation was determined, as shown in Fig. 1. During the experiment, the grinding direction were 0°, 45°, 90°, 135°, 180°, 225°, 270°, 315° along the [100] crystal orientation.

The influence of the anisotropy on tangential grinding force *Ft* and normal grinding force *Fn* of DD5 was investigated using the single factor plane groove grinding experiment, in which the grinding wheel linear speed v_s, the grinding depth a_p, and the feed rate v_f were constant. θ is the angle mentioned above. The single factor experimental design scheme is shown in Table 1.

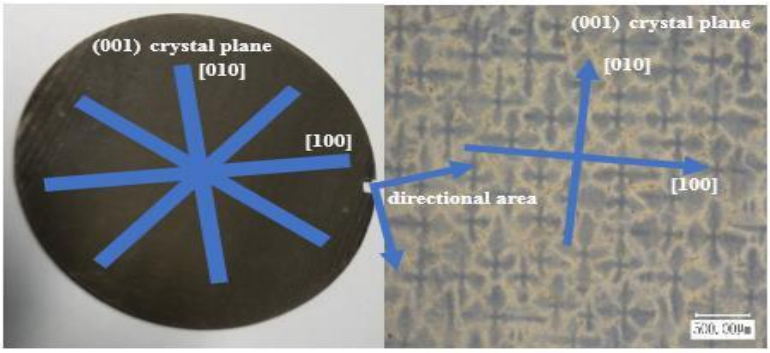

Fig. 1 Crystalline division

Table 1 Single factor experiment of the influence of anisotropy on grinding force

experimental number	v_s [m/s]	a_p [μm]	v_f [m/min]	θ [°]	crystal orientation	tangential grinding force *Ft* [N]	normal grinding force *Fn* [N]
1	25	60	0.6	0	100	9.2	12.8
2	25	60	0.6	45	110	6.7	15.8
3	25	60	0.6	90	010	9.9	14.1
4	25	60	0.6	135	$\bar{1}10$	7.9	16.9
5	25	60	0.6	180	$\bar{1}00$	10.6	13.7
6	25	60	0.6	225	$\bar{1}\bar{1}0$	8.3	16.1
7	25	60	0.6	270	$0\bar{1}0$	9.5	14.9
8	25	60	0.6	315	$1\bar{1}0$	8.1	16.6

Experimental results and analysis. According to the selected grinding wheel linear speed (25m/s), grinding depth (60μm), feed rate (0.6m/min) and the angle θ, a single factor plane

groove grinding experiment of nickel-based single crystal superalloy DD5 was conducted. The tangential grinding force *Ft* and normal grinding force *Fn* in each group were measured by the KISLER 9257B dynamometer. The results are shown in Table 1. The surface morphology after grinding was observed by the VHX-1000E super-depth microscope. According to the experimental results, the influence curves of the angle θ on tangential grinding force *Ft* and normal grinding force *Fn* were drawn respectly, as shown in Fig. 2. The influence of the anisotropy on grinding force of nickel-based single crystal superalloy DD5 was analyzed then.

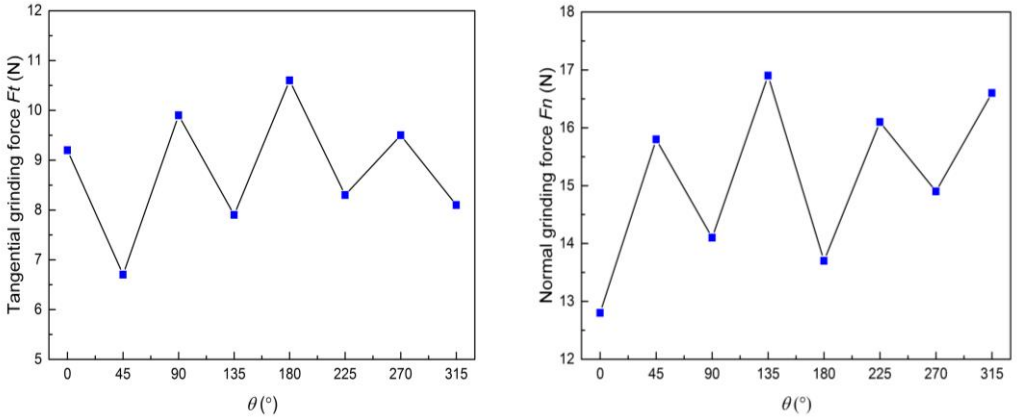

(a) The tangential grinding force *Ft* (b) The normal grinding force *Fn*

Fig. 2 The influence of θ on grinding force

It can be seen from Fig. 2(a) that when the angle θ is 45°, the tangential grinding force *Ft* is the smallest. It can be seen from Fig. 2(b) that when the angle θ is 0°, the normal grinding force *Fn* is the smallest. When the angle θ is 45°, 135°, 225°, 315°, the tangential grinding force *Ft* is smaller than that of 0°, 90°, 180°, 270°. When the angle θ is 0°, 90°, 180°, 270°, the normal grinding force *Fn* is smaller than that of 45°, 135°, 225°, 315°. Analysis of the reasons: From the above Eq. 4, we can know that when the angle θ is 45°, 135°, 225°, 315°, the (001) crystal plane shear modulus $G_{(001)}$ of nickel-based single crystal superalloy is the smallest. From the above Eq. 6, we can know that when the angle θ is 0°, 90°, 180°, 270°, the (001) crystal plane elastic modulus $E_{(001)}$ is the smallest. We can also know from Eq. 4 and Eq. 6 that the (001) crystal plane shear modulus $G_{(001)}$ and elastic modulus $E_{(001)}$ of nickel-based single crystal superalloy change periodically with the cycle of $\pi/2$. The tangential grinding force *Ft* is related to the shear modulus *G*, and the normal grinding force *Fn* is related to the elastic modulus *E*. Therefore, the tangential grinding force *Ft* and the normal grinding force *Fn* also change periodically with the cycle of $\pi/2$. The grinding force of nickel-based single crystal superalloy DD5 exhibits significant anisotropy. The grinding surface morphology when the angle θ = 0°, 45°, 90° is shown in Fig. 3.

(a) θ is 0° (b) θ is 45° (c) θ is 90°

Fig. 3 Grinding surface morphology under different angle θ

Grinding subsurface microstructure. The CA20 low speed wire electric discharge machine was used to cut the experimental workpiece into the subsurface sample with the width of 1 mm. Then the subsurface sample was inserted and polished, and finally the subsurface sample corrosion treatment was conducted. The corrosion liquid composition is $C_3H_8O_3$:HF: HNO_3=10ml:5ml:2.5ml, and the corrosion time is 32s. The Ultra Plus field emission scanning electron microscope (SEM) was used to observe the subsurface sample, as shown in Fig. 4, in which the angle θ is 45°.

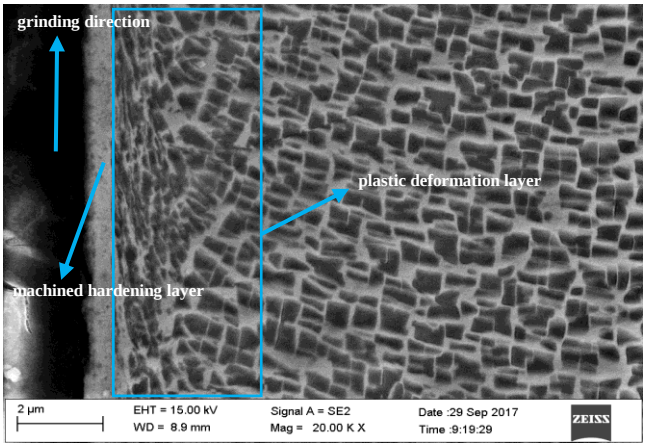

Fig. 4 Grinding subsurface microstructure

It can be seen from Fig. 4 that the nickel-based single crystal superalloy DD5 microstructure is composed of the matrix-γ phase and precipitation phase-γ' phase, and the γ' phase is evenly embedded in the γ phase with a volume fraction of about 70%. When the grinding wheel linear speed is 25m/s, the grinding depth is 60μm, and the feed rate is 0.6m/min, a plastic deformation layer of about 3μm appears on the grinding subsurface, and the γ phase and γ' phase in the plastic deformation layer twist seriously. A machined hardening layer of about 1μm appears between the grinding surface and the plastic deformation layer.

Grinding debris surface morphology. The debris generated in the grinding process reflects the grinding mechanism and the material plastic deformation effectively. The debris collection box was installed on the worktable of the 2M9120 multi-used grinding machine to collect the debris generated in the grinding process. The debris surface morphology was observed with the Ultra Plus field emission scanning electron microscope, as shown in Fig. 5. The contact surface of the debris and abrasive is smooth, and another surface of the debris is free surface. Compared with the contact surface of the debris, the free surface is not continuous, showing the serrated features of a section.

Fig. 5 Grinding debris surface morphology

Conclusions

1. The shear modulus $G_{(001)}$ and elastic modulus $E_{(001)}$ along different crystal orientations in the (001) crystal plane of nickel-based single crystal superalloy change periodically with the cycle of $\pi/2$.
2. When the angle θ is 45°, the tangential grinding force *Ft* is the smallest. When the angle θ is 0°, the normal grinding force *Fn* is the smallest. When the angle θ is 45°, 135°, 225°, 315°, the tangential grinding force *Ft* is smaller than that of 0°, 90°, 180°, 270°. When the angle θ is 0°, 90°, 180°, 270°, the normal grinding force *Fn* is smaller than that of 45°, 135°, 225°, 315°.
3. The plastic deformation layer of about 3μm and the machined hardening layer of about 1μm appear on the grinding subsurface. The grinding debris mainly shows discontinuous and presents the serrated features.

Acknowledgment

This paper's work is supported by the National Natural Science Foundation of China (No. 51375082 and 51775100) and the Fundamental Research Funds for the Central Universities (No. N160306001).

References

[1] Y. D. Gong, Y. G. Zhou, X. L. Wen, J. Cheng, Y. Sun, and L. J. Ma, Experimental study on micro-grinding force and subsurface microstructure of nickel-based single crystal superalloy in micro grinding, J. Mech. Sci. Technol. 31 (2017) 3397-3410.

[2] Q. L. Li, J. H. Xu, H. H. Su, and W. N. Lei, Fabrication and performance of monolayer brazed CBN wheel for high-speed grinding of superalloy, Int. J. Adv. Manuf. Technol. 80 (2015) 1173-1180.

[3] Z. C. Zhao, Y. C. Fu, J. H. Xu, Z. W. Zhang, Z. W. Liu, and J. He, An investigation on high-efficiency profile grinding of directional solidified nickel-based superalloys DZ125 with electroplated CBN wheel, Int. J. Adv. Manuf. Technol. 83 (2015) 1-11.

[4] C. B. Yang, C. G. Lin, H. L. Chiang, and C. C. Chen, Single and multiobjective optimization of Inconel 718 nickel-based superalloy in the wire electrical discharge machining, Int. J. Adv. Manuf. Technol. 93 (2017) 3075-3084.
[5] Q. Li, Y. D. Gong, M. Cai, and M. J. Liu, Research on surface integrity in milling Inconel718 superalloy, Int. J. Adv. Manuf. Technol. 92 (2017) 1449-1463.
[6] T. Sugihara, S. Takemura, and T. Enomoto, Study on high-speed machining of Inconel 718 focusing on tool surface topography of CBN cutting tool, Int. J. Adv. Manuf. Technol. 87 (2015) 9-17.
[7] Y. Z. Lu, G. Xie, D. Wang, S. H. Zhang, W. Zheng, J. Shen, L. H. Lou, and J. Zhang, Anisotropy of high temperature creep properties of a Co-base single crystal superalloy, Mater. Sci. Eng. A. 720 (2018) 69-74.
[8] Y. Mizumoto, H. Kangawa, H. Itobe, T. Tanabe, and Y. Kakinuma, Influence of crystal anisotropy on subsurface damage in ultra-precision cylindrical turning of CaF_2, Precis. Eng. 49 (2017) 104-114.